LABORATORY TECHNIQUES TO CHARACTERIZE NMR DIFFUSION IN CARBONATES

James Funk, Shameem Siddiqui, Mohammed BaTaweel, and Sultan Al-Faqeer
Saudi Aramco Lab R&D Center, Dhahran, Saudi Arabia

Abstract

Petrophysical NMR measurements in carbonate samples illustrate the difficulty of establishing direct size to relaxation rate correlations. Four observations that illustrate this are: T_2 distributions in de-saturated samples that are indistinguishable in fully saturated samples, variations in the T_1/T_2 ratio as a function of relaxation time, saturation dependence of T_2 distributions, and internal gradient effects on T_2 distributions. Additional complications associated with wetting and non-wetting phase fluid saturations are also observed. Complementary tests that clarify these observations and contribute to a more robust modeling of the NMR carbonate response include APEX mercury injection data, CT scan pore volume determinations, resistivity index measurements and de-saturation multi-echo T_2 measurements. Combinations of standard and NMR tests from two carbonate systems, an early Cretaceous marine/lagoon carbonate, and an Upper Jurassic heterogeneous carbonate are used to illustrate how extended laboratory measurements can improve the characterization of NMR response.

Introduction

NMR measurements are based on the surface and bulk interactions of the rock with any hydrogen containing fluid. Measured values are classified by the time-dependent relaxation behavior of the NMR signal. The relaxation process is best described by the equation first proposed by Bloembergen[1].

$$\frac{1}{T_2} = \left[\frac{1}{T_{2_{Bulk}}} + \frac{1}{T_{2_{Diffusion}}} + \frac{1}{T_{2_{Surface}}} \right] \quad \textbf{(1)}$$

When T_1 measurements are made the diffusion mechanism is not active and the corresponding equation is:

$$\frac{1}{T_1} = \left[\frac{1}{T_{1_{Bulk}}} + \frac{1}{T_{1_{Surface}}} \right] \quad (2)$$

In a porous media, the relaxation processes are frequently combined and a single equation is used to relate the relaxation process to the effective surface to volume ratio.

$$\frac{1}{T_2} = r \times \frac{S}{V} \quad (3)$$

The diffusion relaxation is associated with diffusion of spins due to internal or external gradients. It is generally a function of the rock mineralogy, structure, and field strength. The diffusion mechanism is associated with the probability of an excited proton diffusing away from the surface in a time frame shorter than that required for relaxation at the surface. Based on the description of the process by Kenyon[2], a porous media is considered to be in the fast diffusion regime when the diffusion time ($T_{2Diffusion}$) divided by the surface relaxation time is much less than 1. Using this idea:

$$\frac{T_{2\,Difussion}}{T_{2Surface}} = \frac{r^2/D}{r/r} = \frac{r\,r}{D} \ll 1 \quad (4)$$

Values for ρ in carbonates tend to be an order of magnitude lower than those in sandstones and are generally in the range of 0.3 to 3.0 microns/sec. Combined with correspondingly large pores seen in high porosity carbonates, carbonate reservoir rocks would not generally be considered to be in the fast diffusion regime.

Based on the work by Kleinberg[3] and Xu[4], the relaxation due to diffusion is a function of the inter-echo spacing (Tau). In fluids this dependence is proportional to (Tau^2), while in porous media Xu showed that the dependence could be further characterized into a linear range, a range of asymptotic growth, and a plateau range. Xu also showed that for a moderately oil wet rock the rate of change of the T_2 relaxation is a function of the saturating phase.

The effect of the diffusive mechanism is usually considered a nuisance[5]. This is certainly the case when standard permeability estimation models are used. The presence of diffusion results in erroneous characterization of the free fluid and bound fluid indices as well as poorer correlation of permeability with the geometric mean T_2. However, the interactions of fluid, rock, and magnetic field during the diffusion process provide information that is not available without the NMR. Recognition of the diffusion process is the first step. When this is followed with additional NMR experiments and special core analyses, a new tool for petrophysical testing is available.

Experimental

NMR measurements were made on 1.5 in. x 1.5 in. fluid saturated plugs in a Maran 2 MHz NMR instrument. Samples were wrapped in teflon to minimize fluid loss during testing. The NMR signal was acquired using a CPMG (Carr-Purcell-Meiboom-Gill) pulse sequence acquiring 16,000 echoes with inter-echo spacing from 0.1 msec. to 0.9 msec. and a polarization time (delay time) of 7 s. Typically 150 scans were taken with a resulting signal-to-noise ratio greater than 50. The echo trains were processed using a BRD[6] algorithm with the phase-rotated signal. Regularization in the inversion equations was based on the signal-to-noise ratio for each individual sample.

In the Cretaceous carbonate, NMR measurements were made on approximately sixty- (60) samples from three wells as a part of an overall reservoir characterization study. Samples were tested either fully saturated with 180,000 ppm TDS reservoir brine, or at a final irreducible water saturation (S_{wir}) established during resistivity measurement tests. Either the whole core interval or the individual plugs for the samples were CT scanned. Approximately 60 % of these samples were used for additional testing including standard mercury injection tests, APEX mercury injection, or resistivity measurements.

Computerized tomography (CT) scanning was done using a Deltascan-100 scanner (120 kV, 25 mA, translate-rotate system). Post-processing of the images was done using VoxelCalc software on a SUN Ultra-60 workstation. CT number distributions from the scans were converted to porosity distributions and to pore volume weighted porosity distributions normalized to one pore volume. These distributions are referred to as PV-PHI distributions.

APEX mercury injection was done with a CoreTest ASPE 700 System. The system uses a 1cm^3 cubic sample with typical injection rates of 0.00001 cm^3/min. The technique, first described by Yuan[7], allows for measurement of both the pore throat diameter and the pore body diameter.

Resistivity measurements were made on brine saturated plugs using an in-house four lead system. Samples were confined under an effective reservoir stress and desaturated on a water-wet porous plate. Resistivity measurements were made at frequencies from 500 Hz to 20,000 Hz at approximately eight (8) saturation values.

Individual Jurassic carbonate samples were selected from a larger group of samples that had been unprocessed, cleaned or preserved. The collection of samples used had porosities that varied between 14 and 28 percent. The groups of samples had varying saturation and preservation histories that can be classified as:

- Native state
- Cleaned/resaturated
- Wettability-preserved

Stock tank oil from the reservoir (2.41 cP) and 12,500-ppm TDS brine (1.043 cP) were used for resaturation of the native-state and clean/resaturated samples.

The native state samples were part of a conventional core that was not wettability- preserved at the well site. The twelve (12) samples were partially dry with no apparent fluid saturations but all showed external oil staining. Spreading tests of oil and water indicated that the samples were strongly oil-wet. Initial NMR measurements were made on these samples along with NMR measurements after each saturation step listed below.

- Centrifugation to establish the presence of displaceable fluids
- Centrifuge saturation with 12,500 ppm TDS brine

- Desaturation by drying
- Centrifuge saturation with oil
- Centrifuge oil drainage with brine

With the exception of the desaturation by drying, saturations were established in a Beckman Ultra-centrifuge. Samples 1 ½ inch in diameter were saturated or desaturated at rotational speeds up to 7000 RPM in either the standard or inverted buckets.

The cleaned/resaturated and the wettability-preserved samples were tested under single saturation conditions. The cleaned/resaturated samples were from a completed laboratory core flood and were at residual oil saturation (S_{or}). The wettability-preserved sample was selected from a group of ten (10) samples that were drilled under brine from a wettability-preserved whole core near the top of the oil column.

Results

Cretaceous Carbonate

The correlation between the NMR porosities determined by the initial CPMG sequence NMR signal and the conventional porosities is apparent from the data in Table 1. Also apparent is the poorer correlation of permeability based on T_{2lm}, especially with the non-lagoonal facies. Sample #514 is typical of the lagoonal facies. CT images of the sample are shown in Figure 1. The CT number data from the image are converted to porosity and normalized for one pore volume. These porosity distributions and normalized pore volume distributions are plotted in Figure 2. The distributions are Gaussian and indicate that both the porosity and the pore volume are normally distributed about the mean. There are however, positional variations in the porosity and pore volume as indicated by the color variations between slices. The T_1 and T_2 distributions are shown in Figure 3. The distributions are generally log-normal and the ratio of the mean times for the T_1 and T_2 distributions gives 1.2 as the peak T_1/T_2 ratio.

Table 1 – Petrophysical Properties Cretaceous Carbonate Sample

Sample No.	*Facies*	*Porosity (fraction)*		*Permeability (md.)*	
		Conventional	NMR	Conventional	NMR
514	Lagoon	0.254	0.261	11.5	18.2
352	Rudist	0.101	0.093	8.1	0.06
379	Rudist	0.122	0.134	2380	4.5
52	Lagoon	0.248	0.245	4.6	8.6
54	Lagoon	0.269	0.251	7.8	8.4
51	Lagoon	0.258	0.249	4.3	4.5
71	Lagoon	0.230	0.222	5.1	7.1
69	Lagoon	0.256	0.246	9.1	19.5
113	Lagoon	0.216	0.234	7.7	13.0

In Figure 4, the T_2 distribution is plotted with the data from an APEX mercury injection test. The T_2 peak at 126 msec. closely matches the APEX pore body size peak at 125 microns. However, the lower T_2 peak seen at 1 msec. requires a factor of two (2) to match the APEX pore throat peak. As a further complication in the interpretation of surface relaxivity, conventional mercury injections tests were not available on this sample. However, standard mercury injection tests on samples from this facies generally show a mono-modal distribution of pore throat sizes centered at approximately one (1) micron.

For the more heterogeneous samples (non-lagoon facies) from this reservoir, typified by Sample #352, NMR measured porosity agrees with standard porosity when additional handling measures are employed to prevent drainage of surface pores. However, as seen in Table 1, T_{2lm} permeability estimates in this facies can underestimate the permeability by one to three orders of magnitude. Figure 5 shows the slice-by-slice CT image. The porosity and pore volume distributions determined from the CT data are shown in Figure 6. Both figures show the broad distribution of pore volume with porosity for samples from this facies. The long tail above a porosity value 0.21 indicates that a substantial portion of the pore volume in this sample is associated with high porosity regions. The T_1 and T_2 distributions for this sample are shown in Figure 7. Based on the CT pore volume data, it is not surprising to see the long T_1 and T_2 times in the distribution. These times are close to that of the bulk brine. Assuming a correlation between the peaks seen in the T_1 and T_2 distribution, peak T_1/T_2 ratios can be calculated. These are listed in Table 2 with sample 514 used a reference.

Table 2 - T_1/T_2 Ratios for Cretaceous Carbonate Samples

Sample No.	*Peak No.*	*T_1 (msec)*	*T_2 (msec)*	*Ratio*
514	1	148	126	1.17
352	2	11	9.33	1.18
352	3	91.1	77.4	1.18
352	4	1450	246	2.66

Shown in Figure 8 are T_2 distribution curves on two of the lagoonal samples taken on fully saturated plugs and plugs at the lowest saturation in the resistivity test. The differences in the peak T_2 times for two saturation conditions are compared with the saturation exponents for these and other samples in Table 3.

Table 3 - T_2 Saturated and T_2 Desaturated Ratios for Cretaceous Carbonate Samples

Sample No.	*T_2 Peak (msec)*			*Saturation Exponent*
	Saturated	Desaturated	Ratio	
52	148	87	1.7	2.99
54	148	54.6	2.71	2.44
51	107	21.5	4.98	1.90
71	242	26	9.3	1.93
69	148	26	5.7	1.78
113	175	32	5.35	1.78

Jurassic Carbonate

Partially dried native samples exhibited no displaceable oil in the centrifuge but did show the T_2 response seen in Figure 9. Figure 9 also shows the T_2 distributions for the partially dry native sample following brine resaturation. At the initial saturation (partially dried) saturation conditions the T_2 times are short, ranging form 1,000 to 100,000 microseconds with a small integral value. This distribution of short times is still present in the sample after brine resaturation.

These samples were allowed to dry and the experiment was repeated this time using oil as the resaturation fluid. The final step was centrifuge oil desaturation to an Sw value of approximately 30%. Figure 10 shows the T_2 distributions at the shortest echo spacing and the longest echo spacing of these saturation conditions.

Similar multi-echo spacing T_2 measurements are shown in Figures 11 and 12 for one of the cleaned/resaturated samples and one of the wettability preserved samples.

Discussion

Cretaceous Carbonate

As shown in Figure 8 for Sample #113, a key problem with some carbonates is the characterization of an appropriate T_2 cut-off based on the maximum T_2 time for the desaturated sample. Sample #113 is likely to underestimate the T_2 cut-off while Sample #52 is likely to overestimate it. One explanation of the shift in the T_2 distribution curves is a simple lowering of the S/V due to loss of water surface. Straley[8] showed this for desaturation of sandstone samples with kerosene using T_1 distributions. However, the T_1 values for the water-desaturated samples were a part of the original T_1 distribution in the fully saturated samples. This is not the case with these carbonate rocks and their T_2 distributions. Another complimentary explanation for the phenomena is a diffusive loss of spins in the saturated sample. In the desaturated samples where molecules cannot diffuse into the larger pore space, spins are relaxed at a rate established by the S/V of the fluid in the pores. However, in the saturated sample molecules have a fluid volume available for diffusion from the surface to the center of the pore. In this location relaxation of spins occurs at the bulk (generally slower) rate.

Calculation of the diffusion regime for these samples using Equation (4) is dependent on the values of ρ and the choice for r. With ρ = 1micron/msec determined from APEX pore body measurements, r = 1 micron from standard mercury injection tests, and D=2.0 x 10^{-5} cm^2/sec, the ratio ($\rho * r/D$) is 0.0005. This would indicate that the sample could be in the fast diffusion regime. An alternate choice for r based on the APEX pore throat data would provide a similar fast diffusion regime estimate. However, if r is considered as the S/V ratio from the APEX pore body data (r = 125 microns), the new value for the ratio ($\rho * r/D$) is 0.062, which would no longer be considered in the fast diffusion regime.

As seen in Figure 6, one characteristic of the CT pore volume distribution is the long tail at higher porosity values. Assuming that the pore volume distributional tail is reflective of the larger pore sizes, the T_1/T_2 comparison seen in Table 2 can be used as a qualitative tool to estimate the diffusive contribution. In the less heterogeneous Sample #514, the ratio (T_1/T_2) is approximately 1.2 as is the ratio for the shorter times in Sample #352. However, the ratio (T_1/T_2) is increased to 2.66 for the longer times and the pore space characterized by the long PV-PHI tail.

The results in Table 3 illustrate how additional special core analysis data such as electrical property measurements can be used to characterize the diffusive response in lagoonal carbonates. Samples with higher saturation exponents have a less conductive saturation dependent path available for the flow of current. In brine-saturated samples desaturated by air, the path is established by the location and the connectivity of the brine phase. Continuous films of brine will be more conductive than disconnected regions of brine. A similar surface relation to conductivity has been established for microporosity[9,10].

As seen in Table 3, samples with the largest ratio for saturated/desaturated T_2 times have the lowest saturation exponent. If the reduced T_2 times correspond to surface films, and these in turn are functioning like microporosity, the NMR diffusion process is providing a characterization of the conductive path with desaturation. A possible mechanism is that samples with the largest ratio for saturated/desaturated T_2 times can be considered as those that desaturated via a surface film, where the volume of the film is reduced with desaturation. The film remains continuous through out the desaturation. In contrast, samples that show less shift in the T_2 spectrum to lower times with desaturation (and smaller ratios for saturated/desaturated T_2 times) have less of this surface film desaturation. With this mechanism the surface film desaturated samples would show less of a change in resistivity than would samples that desaturated entire pores.

Jurassic Carbonate

At present, our characterization of diffusion in carbonates with two liquid phase saturations is more qualitative than quantitative. In the case of the Jurassic carbonate that was studied, the T_2 times for the oil (120 msec.) and the brine (1.4 sec.) at room temperature also influenced the interpretation.

A comparison of the T_2 distributions for the partially dried native state and the brine saturated native state Sample # 1131 in Figure 9 indicate that the brine within this sample is generally relaxing at a rate that is slightly lower than the rate for the bulk brine and the oil is responding as it did in the partially dried condition. The shaded distribution contains a slightly shifted original oil distribution and a substantially shifted brine distribution. The shifted oil distribution may be the result of some redistribution of oil into smaller pores. The shifted brine indicates that even in this oil wet sample surface relaxation of the brine is present.

The results of a repeat of the experiment, this time with resaturation with oil, are shown in the oil-saturated distribution in Figure 10. The probable oil film that was apparent in Figure 9 (low T_2 times) is no longer apparent and a single oil T_2 distribution seen. When a portion of

the oil is displaced by brine (oil and brine saturated with $S_w \approx 30\%$) there is little surface area for brine surface relaxation and the added brine relaxes at a rate close to its bulk rate.

If variable echo spacing is used to quantify the diffusive effect preservation and possible wettability effects are seen. Under the two saturation conditions for the native state sample in Figure 10, there is little shift in the distributions at increased echo spacing. A similar result is seen in Figure 11 for the dominant T_2 peak in the cleaned/resaturated Sample #157. However, in the wettability preserved Sample #8, the peak that would be assigned to the bulk brine is not present at the longer echo spacing. No clear mechanism for the interaction is apparent and additional tests are needed to clarify this saturation, wettability, and diffusive interaction.

Conclusions

Laboratory NMR measurements in carbonates provide a unique look at the interaction of pore fluids with reservoir rock fabric. However, the characterization of this response requires an understanding and quantification of different interaction mechanisms. The least described of these is the diffusive mechanism. Use of additional petrophysical tools in combination with NMR provides a perspective on the mechanism and phenomenological descriptions of current NMR petrophysical models. Our study illustrated that:

- Use of a diffusivity "rule of thumb" to estimate the diffusion regime requires a consistent basis for both the surface relaxivity ρ and the characteristic pore size r.
- CT number distributions can be interpreted with NMR T_2 distributions to provide a tool for characterization of the maximum diffusive response.
- Electrical property measurements support a conceptual model of surface film desaturation in carbonates.
- Two-phase saturation effects provide a qualitative contrast that impacts the assessment of wettability effects on T_2 distributions and T_2 diffusion.

When the relaxation process is not a simple surface phenomenon, other techniques are needed to accurately describe the pore space and hopefully correlate petrophysical properties. An experimental protocol that uses information derived from complementary techniques is the best approach. One such protocol can be:

1. Identification of the deviations and/or exceptions to current physical models for NMR response based on conventional and special core analyses.
2. Selection of tests to address pore size and pore volume relationships.
3. Additional NMR tests to refine or remodel NMR response.

This combination of tests provides a petrophysical synergy that is essential to understanding and developing robust carbonate models.

Acknowledgments

The authors wish to acknowledge the Saudi Arabian Oil Company (Saudi Aramco) for granting permission to present and publish this paper. We would also like to acknowledge Mr. Jack Lynn and Mr. Mohammad Alqam of the Formation Damage Group for providing the APEX data.

Nomenclature

T_{2lm} = *Log Mean T_2 time*

T_2 = *Transverse Relaxation Time*

$T_{2\,Bulk}$ = *Bulk Relaxation Time*

$T_{2\,Surface}$ = *Surface Relaxation Time*

$T_{2\,Diffusion}$ = *Diffusion Relaxation Time*

ρ = *Surface Relaxivity*

D = *Bulk Fluid Diffusion Coefficient*

r = *Characteristic Pore Size*

S/V = *Surface to Volume Ratio*

References

1. Bloembergen, N., Purcell, E. M., and Pound, R. V.: "Relaxation Effects in Nuclear Magnetic Absorption," *Physics Review*, 1948, **73**, 679.

2. Kenyon, W. E.,: "Petrophysical Principles of Applications of NMR Logging," *The Log Analyst***,** March-April 1997, **Vol. 38, No.2**, 21.

3. Kleinberg, R. L. and Vinegar, H. J.: "NMR Properties of Reservoir Fluids," *The Log Analyst*, November-December, 1996, **Vol. 37, No.6**, 20.

4. Xu, X. and Davis, L. A.: "The Relation of Pore Size to NMR T_2 Diffusion Relaxation in Porous Media," SPE 56800, Presented at the 1999 SPE Annual Technical Conference and Exhibition in Houston, Texas, 3-6 October 1999.

5. Straley, C., Rossini, D., Vinegar, H., Tutunjian, P., and Morriss, C. E.: "Core Analysis by Low-Field NMR", The Log Analyst, **Vol.38, No. 2**, March-April 1997, 84 .

6. Butler, J. P., Reeds, J. A., Dawson, S. V.: "Estimating Solutions of First Kind Integral Equations with Nonnegative Constraints and Optimal Smoothing,**"** *SIAM J. NUMER ANAL.*, 1981, **Vol. 18, No. 3**, 381.

7. Yuan, H. H., Swanson, B. F.: "Resolving Pore-Space Characteristics by Rate-Controlled Porosimetry," *SPE Formation Evaluation*, **Vol. 4, No. 1**, March 1989, 17.

8. Straley, C., Morriss, C. E., Kenyon, W. E., and Howard, J. J.: "NMR in Partially Saturated Rocks: Laboratory Insights on Free Fluid Index and Comparison with Borehole Logs," *Tran. SPWLA Annual Log. Symposium*, Society of Professional Well Logging Analysts, Paper CC, 1991.

9. Swanson, B.F., "Microporosity in Reservoir Rocks: Its Measurement and Influence on Electrical Resistivity," *The Log Analyst*, **Vol. 26, No.4**, November-December, 1985.

10.Worthington, P.F., Pallatt, N., and Toussaint-Jackson, J. E., "Influence of Microporosity on the Evaluation of Hydrocarbon Saturation," *SPE Formation Evaluation*, June, 1989,**Vol. 4, No. 2**, 203.

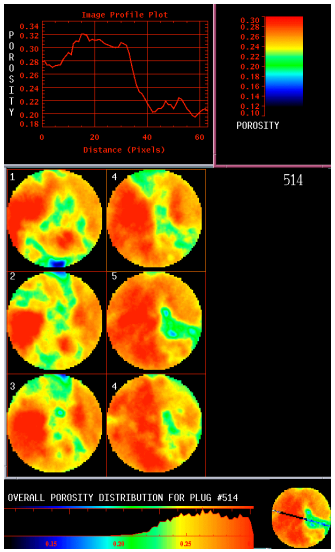

Figure 1 - CT Image for Cretaceous Carbonate (Sample #514)

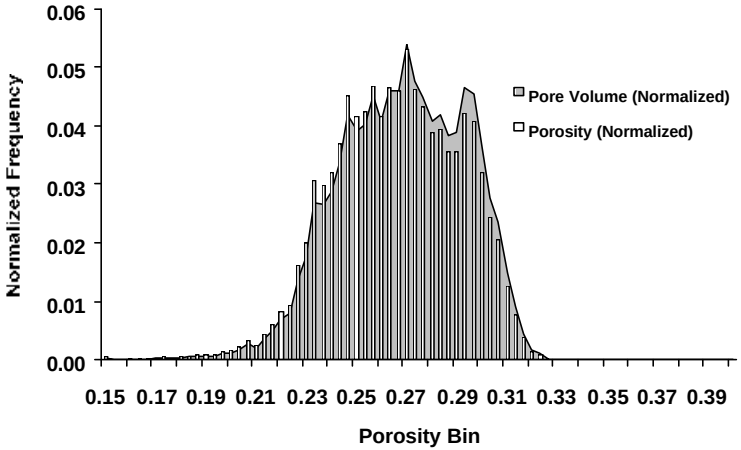

Figure 2 - CT Derived Porosity and Pore Volume Weighted Distributions (Sample #514)

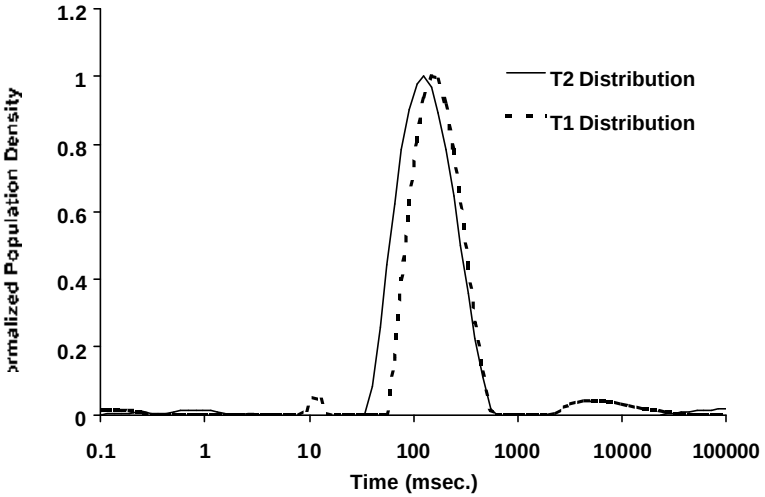

Figure 3 - T_1 and T_2 NMR Population Distributions (Sample # 514)

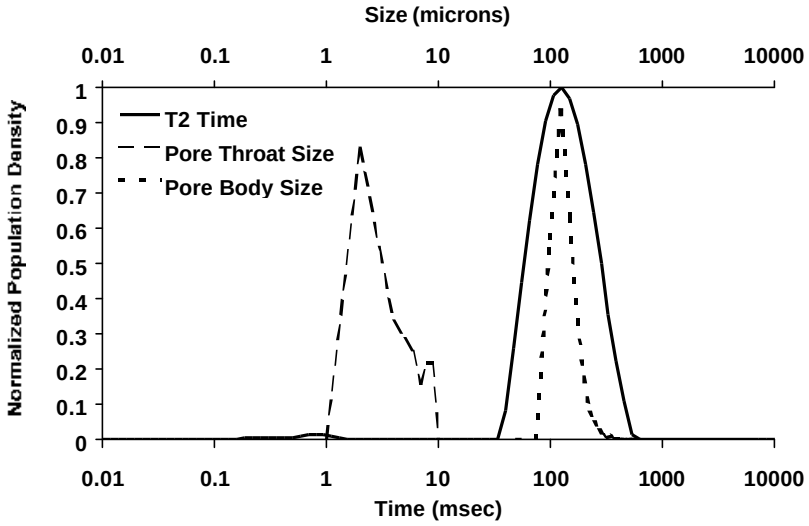

Figure 4 - T_2 Time and APEX Size Distributions (Sample # 514)

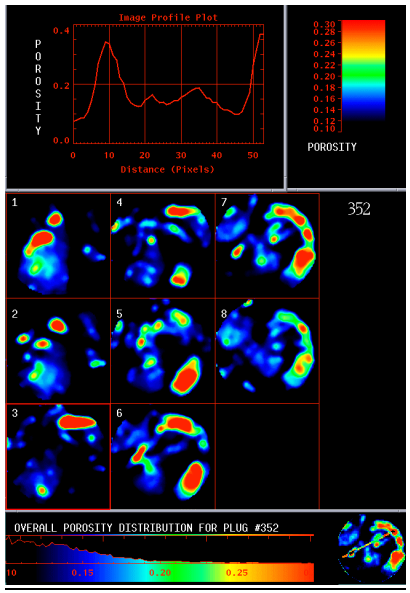

Figure 5 - CT Image for Cretaceous Carbonate (Sample #352)

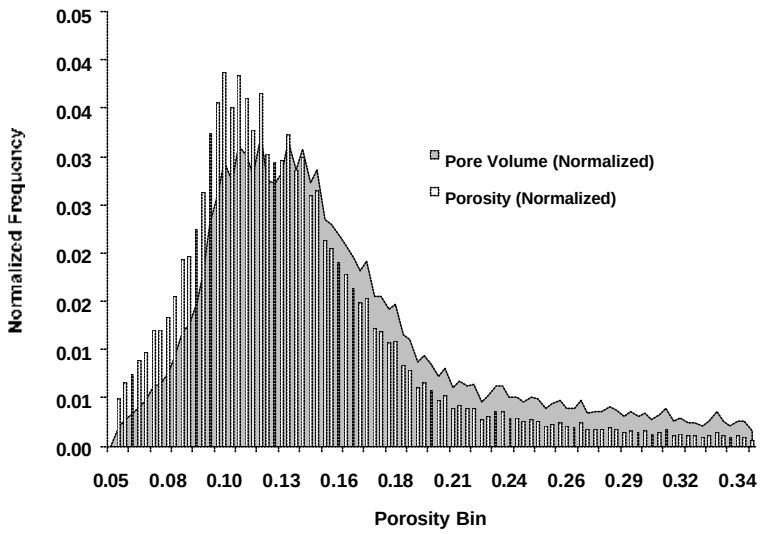

Figure 6 - CT Derived Porosity and Pore Volume Weighted Distributions (Sample #352)

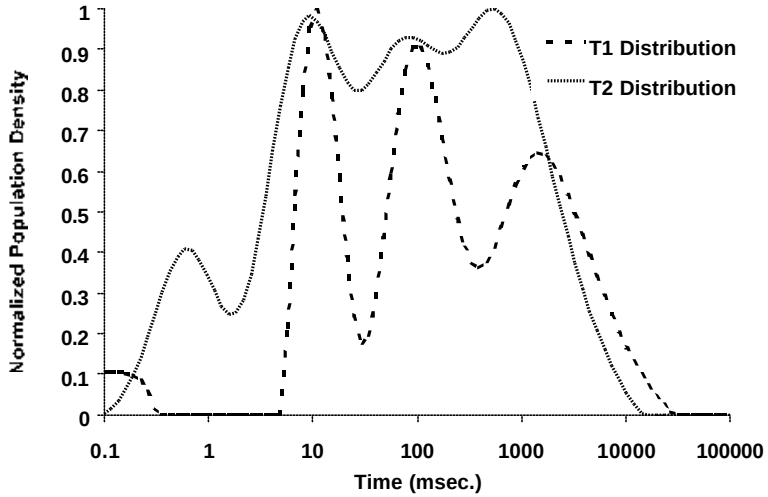

Figure 7 - T_1 and T_2 NMR Population Distributions (Sample # 352)

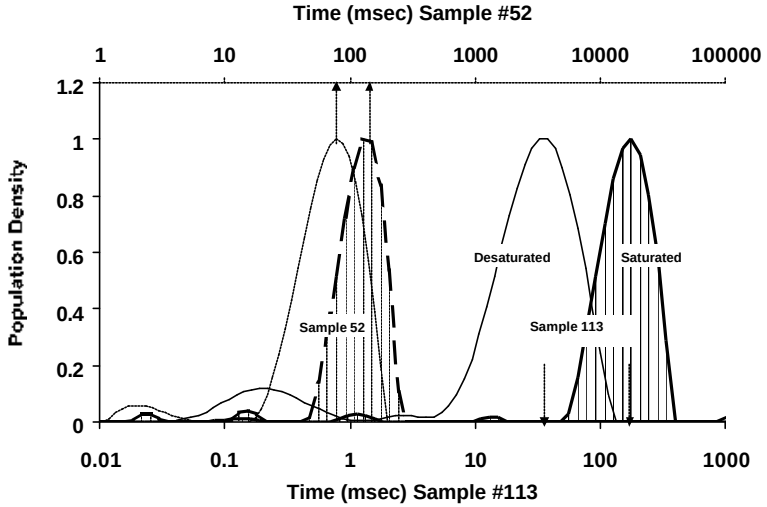

Figure 8 – Desaturation T_2 Time Shifts (Samples #113 and 52)

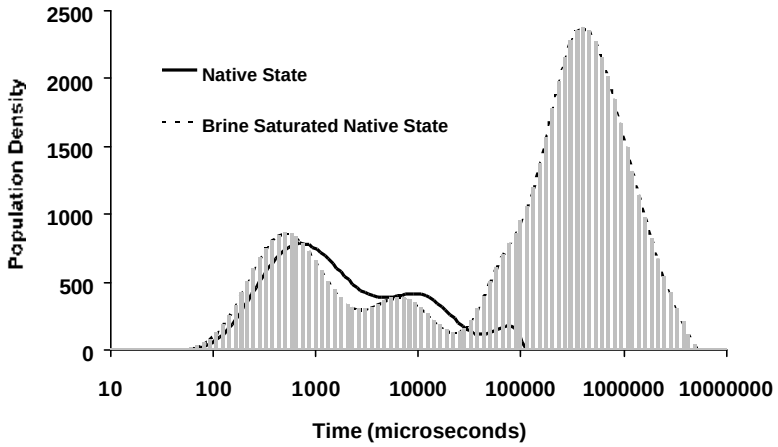

Figure 9 – Jurassic Carbonate Native State and Brine Saturated Native State T_2 Distributions (Sample #1131)

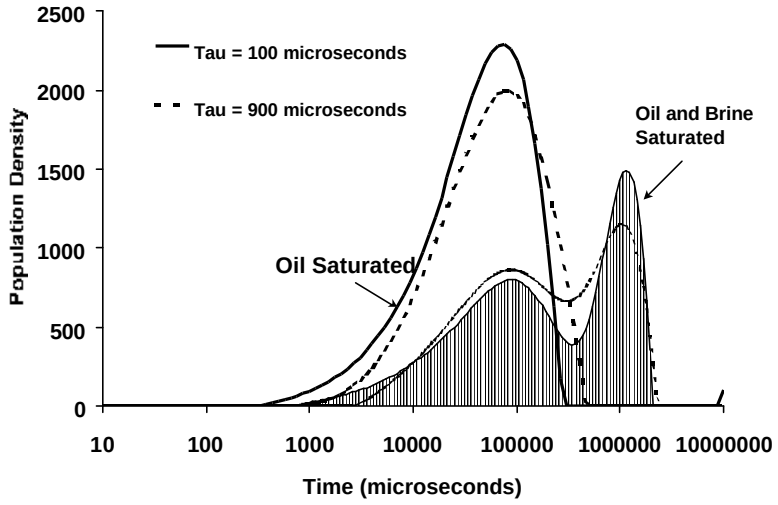

Figure 10 – Oil Saturated and Brine Saturated T_2 Distributions (Sample #1131)

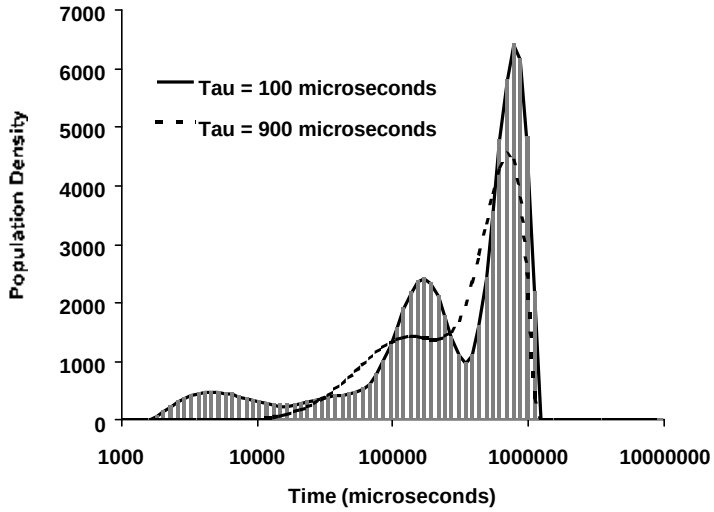

Figure 11 – Cleaned/Resaturated Sample Multi-Echo Spacing T_2 Distributions

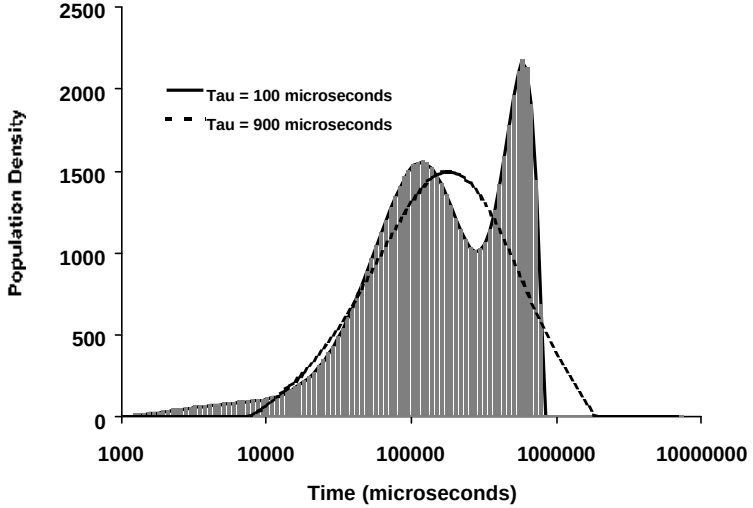

Figure 12 – Wettability Preserved Sample Multi-Echo Spacing T_2 Distributions (Sample #8)